Composites Part C: Open Access 1 (2020) 100009

Contents lists available at ScienceDirect

Composites Part C: Open Access

journal homepage: www.elsevier.com/locate/jcomc

Constructing pristine and modified cellulose nanocrystals based cured polychloroprene nanocomposite films for dipped goods application

Hormoz Eslami, Costas Tzoganakis, Tizazu H. Mekonnen*

Department of Chemical Engineering, University of Waterloo, 200 University Avenue, E6 - 5010 N2L 3G1 Canada, Waterloo, ON, Canada

ARTICLE INFO

Keywords:
Cellulose nanocrystals
Dipped Products
Gloves
Polychloroprene
Curing

ABSTRACT

In this work, polychloroprene rubber (CR) nanocomposite films reinforced with native and modified cellulose nanocrystals (CNCs) were evaluated for dipped goods applications. The CNC modification, with a goal of enhancing the interaction between the CNC and CR, was conducted by surface graft polymerization of lactic acid. The films were then prepared by latex blending, casting, and curing (with ZnO/MgO). TEM studies displayed that the CNCs formed a partially structured network while modified CNCs (mCNCs) tend to disperse mostly individually in the polychloroprene and show percolation at 3 wt%. Tensile tests of the films showed a substantial increase in the modulus, tensile strength, and tear resistance for both CNC, and mCNC reinforced films while the elongation at break remained above 600%. The films made with CNCs and mCNCs exhibited similar acetone vapor permeability at different loadings of the filler. However, their permeability towards water and 2-propanol vapor increased steadily with an increase in CNCs loading. In contrast, the mCNC-based films displayed steady permeability and a surge at 3 wt%, which could be attributed to percolation. Overall, the fabrication of CNC and mCNC reinforced CR films demonstrated appealing physical properties for a range of dipped goods applications.

Introduction

Polychloroprene rubber (trans-1,4- polychloroprene, or CR) has been commercially available in latex form since 1931 [1]. DuPont developed the emulsion free radical polymerization process of 2-chloro-1,3-butadiene to produce CR to replace natural rubber (NR). CR has chlorine atoms that make it chemically resistant to oxidizing agents (oxygen and ozone) and fire. It is also physically polar with good electrical properties, low permeability to gas, and resistant to aliphatic hydrocarbons, chlorofluorocarbons (CFCs), mineral oil, fat, and grease [2]. CR has other notable properties like surface adhesion, resistance to soil bacteria and fungi, and wide service temperature of −35 to −100 °C that make it the preferred choice for demanding applications such as rubber parts [3,4], extrusion profiles and sheets, adhesives, and sealants [5], etc. CR in rubber parts can be used in several applications ranging from swimsuit used in deep ocean water applications (DOWA) to aircraft parts like weather seals, window channels, and parts used in contact with air conditioning fluid, or sealers, washers, and diaphragms in the fuel system [6].

CR is usually cured with a system containing ZnO (Fig. 1) curative and MgO that is not involved in the cure but is added to neutralize the byproducts ($ZnCl_2$). As ZnO shows eco-toxicity towards marine life [7], some studies have focused on reducing the ZnO consumption by precipitating it on other substrates like nano-silica [8], or graphene [9], or inclusion in nano-clay [10–12]. Two groups [11,13] used ZnO nanoparticles (ZnO-N) and MgO nanoparticles (MgO-N) or ZnO-N/MgO-N system directly for curing CR which almost halved the ZnO consumption. A similar system has also been used for curing CR foams [6]. MgO-N/ZnO-N system has also been shown to provide good UV protection [14] and enhance antibacterial properties of the final products used for gloves [15]. Additionally, these nano-metal oxides improve the transparency of products by reducing scattered light attributed to their nanostructure and allowing to reduce the required loading to achieve similar crosslinking as macro-sized metal oxides.

Some studies have also focused on improving the mechanical properties of CR. It is worth mentioning that the field of rubber nanocomposites is in its infancy and barely enough publications are available to establish a strong understanding of their behavior. The literature has been covered in two reviews [16–18] and the nanoparticles used for other polar rubbers might be used to improve the mechanical properties of CR as well. The addition of low-density nanoparticles is the best way to enhance the modulus, tensile strength, and tear strength without sacrificing the density (960 kg/m^3 for green unfilled CR). Some nanoparticles can also improve the aesthetic problems like unwanted tint or color, which is of paramount importance for applications like masks and gloves in which the visual inspection is an essential safety procedure. Ideally, the nanoparticle can be conveniently added to CR latex immediately after the latex production, which makes it suitable for dipped products.

* Corresponding author:
E-mail address: tmekonnen@uwaterloo.ca (T.H. Mekonnen).

https://doi.org/10.1016/j.jcomc.2020.100009
Received 26 May 2020; Received in revised form 25 July 2020; Accepted 28 July 2020

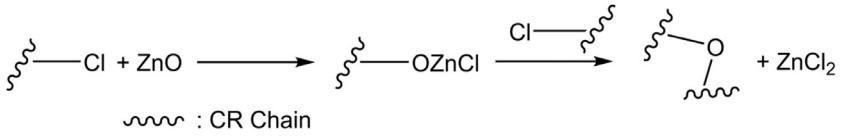

Fig. 1. The schematic of CR cure with ZnO curing system.

Das et al [19] studied the properties of the CR nanocomposites with montmorillonite (MMT) clay and layered double hydroxide (LDH) which were modified with organic modifiers, and found that the clays can result in partial deactivation of the curing agents, and slower curing process. They also found that by adding clay fillers, tan δ in Dynamic Mechanical Analysis (DMA) became smaller for the nanocomposites compared to the CR-Gum sample with no nano-clays indicating reinforcement.

Roy et al [20] studied the effect of silica-coated nano-calcium carbonate (SNCC)/CR nanocomposites on the mechanical properties compared to those of non-coated nano-calcium carbonate (NCC) in order to use inexpensive SNCC in polymers. They found that SNCC/CR nanocomposites, had better curing, and mechanical properties like tensile strength (~41% increase), and Young's modulus (~ 34 % increase), and improved thermal stability. They attributed the observation to the better distribution of SNCC in the matrix due to the improved interaction of silanol groups on the surface of the SNCCs with CR. Abbas et al [21] used reversible addition-fragmentation chain transfer polymerization of CR on the surface of nano-silica with two surface graft densities of 0.022 and 0.210 chains per nm^2. They found that the dispersion of the nano-silica and the mechanical properties of the nanocomposites made thereof improved for the solvent cast cured sheets compared to those of the sample made from non-grafted nano-silica particles. The incorporation of carbon nanotubes [22], and graphene oxide in CR [23] have enhanced the mechanical properties and especially Young's modulus.

Cellulose nanocrystals (CNCs) are appealing reinforcing agents for CR latex because of their good dispersibility in water-based latexes [24]. Moreover, CNCs are renewable, biodegradable, low density, colorless, stiff, naturally abundant with good gas impermeability with the potential to replace conventional nanomaterials used in the polymer industry [25–27]. CNCs form stable water dispersions and can be mixed with CR or other rubber latexes easily as opposed to most other polymers, which are typically non-polar. CNC in non-aqueous media or non-polar polymers suffer from agglomeration, and hence they usually need compatibilizers and/or special surface treatments for their successful incorporation [28]. Various methods like surfactant modification [29] and polymer grafting-to [30] have been investigated to enhance their dispersion in polymer matrices. Fahma et al [31] prepared acetylated cellulose nanofibers (CNFs) from oil palm empty fruit and dispersed them in dichloromethane and mixed the suspension with chloroprene rubber solution in dichloromethane and used the dispersion to cast green films of CNF/CR nanocomposites. The addition of 1, 3, and 5 wt% CNFs resulted in an increase in the strength and Young's modulus. However, the solution cast approach is costly and detrimental to the environment, because of the use of halogenated chemicals (e.g. dichloromethane).

In a previous paper [32], a grafting – from approach for the hydrophobic tailoring of the surface of CNCs that led to a remarkable dispersion improvement in green chloroprene rubber (CR) has been reported (Figure S1). This modification has targeted partial substitution of the surface –OH groups of the CNCs with polylactic acid (PLA). This has resulted in modified CNC particles (mCNCs) of dual nature with mutual dispersibility in aqueous media as a result of the –OH group, and non-polar solvents due to the grafted PLA. The mCNCs also created hydrophobic films upon drying (Fig. S2 in Supporting Information). In the same study, mechanical tests indicated that the incorporation of the CNCs in the CR caused a substantial enhancement in the tensile strength (250%) and modulus (450%) as compared to the control CR films with no fillers. However, this study was limited to uncured (green) chloroprene rubber films, and the results cannot represent practical CR films, which should be cured to be used for real-life applications.

In this work, the effect of native and modified CNCs (CNCs and mCNCs) on the performance of ZnO-cured CR nanocomposite film properties is investigated. The developed films can have useful applications in gloves, membranes, catheters, balloons, etc. Currently, the production of latex gloves, natural rubber, or synthetic rubber-based gloves is dominated by Southeastern Asian countries because of geographic suitability, with natural rubber trees (*Havea brasiliensis)* growing in the region: the industrial capacity has been built up around this plant, resulting in established production facilities and expertise. For instance, Malasia produces about 67% of the gloves used globally [33]. The concern with allergic reactions to NR-based gloves as a result of residual proteins requires the widespread use of alternative materials, such as acrylonitrile-butadiene rubber (NBR) and CR [34], which can also be produced in diverse geographies in addition to South East Asia. The reinforcement of CR with CNCs could pave the way for the production of stronger CR gloves and prevent their premature tearing and squandering with the possibility of self-disinfection and reusability [35]. We believe that this work is the first investigation on the use of CNCs and tailored CNCs as a reinforcing additive of cured CR composite films.

Experimental

Materials

Never-dried cellulose nanocrystal (CNCs) aqueous dispersion (8.4 wt%) with a crystallinity of 88% was supplied by CelluForce Inc. (Montreal, QC, Canada). Toluene (> 99%), KBr, chloroform (99 %), 2-Propanol, L-lactide, and nano-zinc oxide dispersion (ZnO-N, 99+% metals basis, average particle size <100 nm, and 20 wt% in water) were obtained from Sigma-Aldrich. Tin (II) 2-ethylhexanoate ($Sn(Oct)_2$, 98 %), methanol (99%), ethanol (99 %), ammonia solution (7N in methanol), acetone (99 %), and nano-magnesium oxide (MgO-N, 99+% metals basis, and average particle size <100 nm) were obtained from Fisher Scientific. Polychloroprene (Neoprene) latex was sourced from Chemionics Corporation (Tallmadge, Ohio, USA). Reagents were used as received without further purification and modifications. Zinc oxide dispersion was thoroughly shaken before weighing every time.

Grafting – from modification of cellulose nanocrystals

CNC water dispersions was first solvent exchanged with first acetone and subsequently with toluene through a serious of centrifugation, re-dispersion, solvent decantation as described in previous publications [32,36,37] to carry out the reaction. Briefly, the CNC water dispersion was first diluted five times with the addition of acetone, mixed, and centrifuged (4000 rpm, Thermofisher, Megafuge Centrifuge, USA), the supernatant solvent was decanted, and the residue was re-dispersed in acetone using a homogenizer (PowerGen 700, Fisher Scientific, USA). This process is repeated three times to ensure that the water is replaced with acetone. Additional solvent exchange was conducted to replace the acetone with toluene following the same steps.

Dispersion of 4 g CNC in 200 mL of toluene was prepared and transferred to a 250 mL round-bottom two-neck flask, followed by the addition of $Sn(Oct)_2$ catalyst (0.04 g). The flask was placed in an oil bath, the temperature was raised to 100 °C, and the monomer (2 g, L-lactide) was added under intense agitation using an overhead mixer to carry

Table 1
Recipes for the cured rubber samples. The numbers are stated on a dry-rubber-basis which is the rubber formed from that latex (61.4 w% solid) after the completion of the drying process.

Sample code	CR (phr) (dry-basis)	ZnO-N (phr) (Nano ZnO)	MgO-N (phr) (Nano MgO)	CNC (phr)	mCNC (phr)
CR	100	2.5	2	-	-
0.5CNC	100	2.5	2	0.5	-
1CNC	100	2.5	2	1	-
2CNC	100	2.5	2	2	-
3CNC	100	2.5	2	3	-
0.5mCNC	100	2.5	2	-	0.5
1mCNC	100	2.5	2	-	1
2mCNC	100	2.5	2	-	2
3mCNC	100	2.5	2	-	3

out the graft modification reaction. The reaction was allowed to proceed overnight. Subsequently, the reactor was cooled down to room temperature using an ice bath, and the modified CNCs were separated via centrifugation. The modified CNCs were washed using warm chloroform (50 °C, 3 times) to remove unreacted lactides, oligomers, and ungrafted polymer chains[32]. Complete removal of the unreacted lactides, oligomers, and PLA was confirmed by infrared analysis of the chloroform from the last washing step.

Characterization of the modified CNCs

Fourier transform infrared spectroscopy

The level of CNCs modification was qualitatively and quantitatively evaluated using infrared spectroscopy (FTIR) (Nicolet FTIR 6700, ThermoFisher Scientific, USA). For this, about 2 mg dried powder of the pristine CNCs, PLA grafted CNCs, and native PLA were pressed into pellets together with KBr powder (1:100 ratio). FTIR spectra in absorbance mode were then acquired. To calculate the quantity of grafted PLA on the surface of CNCs, a calibration curve was developed as reported in another study [32].

PLA content determination

The ester value was used to determine the PLA graft content in the modified CNC as per ASTM D5558 with slight modification. Potassium hydroxide (4 g) was added to dry ethanol (40 mL) and was dissolved until a clear solution was formed. The dried mCNC sample was then added to the solution. The resulting dispersion was boiled under reflux for 30 min and mixed for two weeks to ensure that the saponification reaction was complete. The ester value was then measured by back titration with hydrochloric acid. The titration was repeated for three consecutive days and the completion of saponification was confirmed when a constant ester value obtained.

Fabrication of polychloroprene film and curing

The native and modified CNCs were incorporated in the film formulation to fabricate the polychloroprene film. For formulations containing native CNCs, 2 wt% of native CNC dispersion prepared by diluting the masterbatch CNC dispersion. In the case of mCNCs, the modified sample was dried, ground, and redispersed in water. Aqueous dispersions of MgO-N (2 wt%) were prepared by adding water to dry MgO-N, and aqueous dispersions of ZnO-N (2 wt%) were prepared by adding water to 20 wt% aqueous dispersions of ZnO-N. All the dispersions were homogenized and sonicated for 2 min each before adding to the latex. Calculated quantities of the CNC and mCNC dispersions were mixed with the polychloroprene latex (61.4 wt%) to obtain CR (control CR with no CNC), 0.5CNC, 1CNC, 2CNC, and 3CNC samples that are cured CR samples with 0.5, 1, 2, 3 wt% CNCs, respectively. Similarly, 0.5mCNC, 1mCNC, 2mCNC, and 3mCNC CR nanocomposite films were prepared that contain 0.5, 1, 2, 3 wt% mCNC as shown in Table 1. Each formulation was homogenized (2 min) and ultra-sonicated (2 min), followed by slow overnight mixing with a magnetic stirrer. The viscosity of the CR latex, containing no cellulosic nanoparticles, was measured to be 21.5 cp. The required amount of MgO-N, and ZnO-N dispersions were then added to the latex mixture with extra water to keep the final viscosity at 21.5 cp (within ±10%; Table S1 in Supporting Information). Finally, the dispersions were further homogenized and sonicated (each for 2 min), degassed to remove air bubbles, and cast on clean, Pyrex glass molds at room temperature. The sample specimens were allowed to dry at room temperature for at least two days, removed from the mold, and left for 24 extra hours to dry at ambient temperature. The samples were then vulcanized in an oven at 150 °C for 7 min, and the resulting cured nanocomposites were cut and used for the tensile, tear, DMA, and solvent transmission tests.

CR nanocomposite film characterization

Tensile test

For tensile testing, cured films were cut into strip test specimens (70 mm × 10 mm) and conditioned according to ASTM D882 (10 mm × 70 mm). The tensile test was then carried out on five specimens using a Tensile Testing Equipment (AGSX Shimadzu, Japan) equipped with 1 kN load cell, at a speed of 500 mm/min.

Tear test

For tear testing, sample specimens were conditioned and cut from the constructed films according to ASTM D624-12 with some modifications. The trouser tear test samples type T (15 mm × 70 mm) were cut from the films, and three samples from each batch were tested using a Tensile Testing Equipment (AGSX Shimadzu, Japan), equipped with 1 kN load cell at a speed of 50 mm/min, and the average was reported.

Transmission electron microscopy

For transmission electron microscopy (TEM) analysis, cryo-cut specimens (100–150 nm thickness) were prepared using a cryo-ultramicrotome (Leica, EM FC7) and placed onto 100 mesh Formvar-coated Cu grids. TEM micrographs were then taken from the sections with a JEOL 1200EX TEMSCAN equipped with an AMT Digital Camera (4 megapixels) using an acceleration voltage of 80 kV.

Moisture and solvent vapor transmission

Moisture and solvent barrier properties of the thin films were tested to determine the effect of CNC on the permeability of latex according to ASTM E96 for the water vapor transmission of materials [38]. The solvent or water was added to glass cups and the films were tightly secured to the mouth of the glass cups to ensure that the water or solvent loss is only through the films. The glass cups were weighed immediately and at least once every day for seven days. The water and solvent vapor transmission (SVT) was calculated using Eq. (1).

$$SVT = G/t \cdot A \quad (1)$$

where G is the weight change in grams, t is the elapsed time in hours, and A is the area of the cup mouth in m^2. A graph of weight loss versus time was then developed and the slope was used to calculate the transmission rate [39,40].

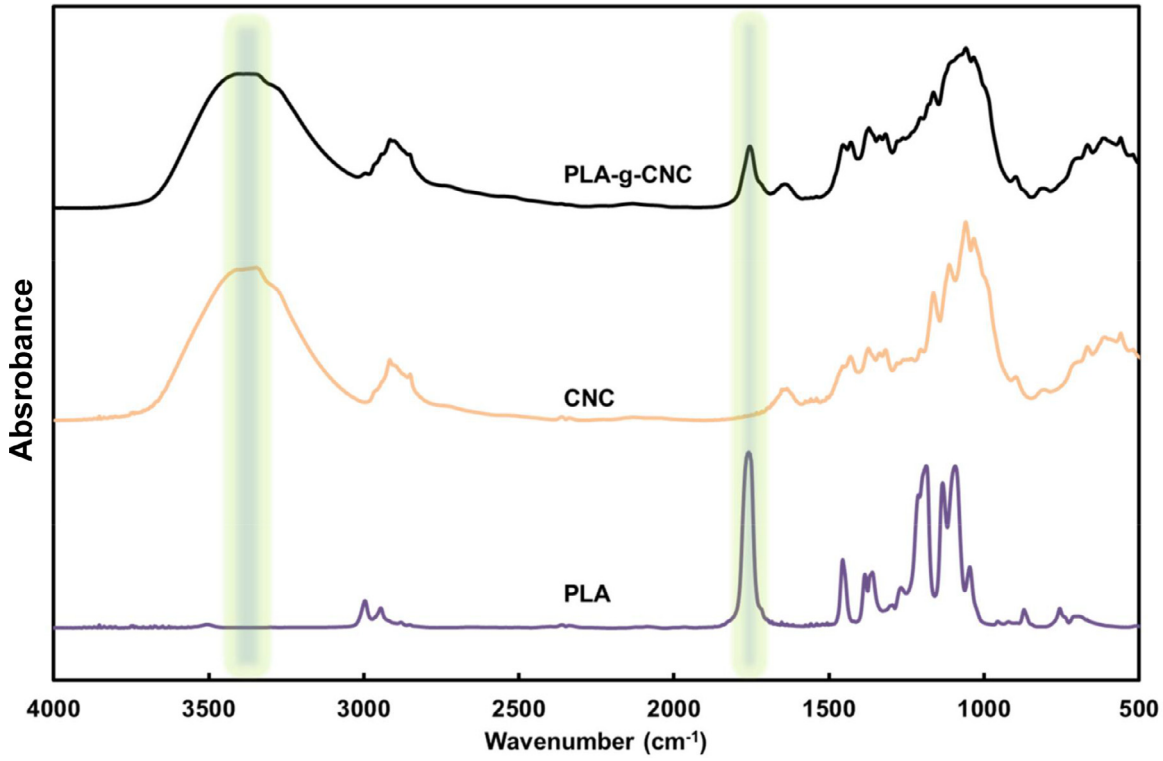

Fig. 2. IR spectra of native CNCs, PLA, and mCNC.

Results and discussion

CNCs modification

CNCs were modified by the graft ring-opening polymerization of (L)-lactide as described in detail elsewhere [32] to produce PLA grafted CNCs (mCNC, Figure S1 in Supporting Information). Fig. 2 presents the FTIR spectra of the control PLA, control CNC, and the modified CNCs (mCNCs) produced in this work. PLA has an easily distinguishable peak at 1780 cm^{-1} [41] for C=O stretch vibration (together with that of 1680 cm^{-1}) and native cellulose nanocrystals have a characteristic peak at 3451 cm^{-1}, which is assigned to O–H (together with that of 2900 cm^{-1} for C–H stretching vibration). These peaks were used for quantifying the PLA contents on the mCNC. The IR estimation showed 11.4 wt% of PLA in comparison to the total weight of the mCNCs. The PLA content was also estimated by measuring the ester value and the result was 12.4 wt% from triplicate measurements, which is the same order of magnitude as that of the measurement obtained from IR estimation

Differential scanning calorimetry (DSC) of the mCNC revealed a glass transition temperature (T_g) at 61.3 ˚C which was missing in the DSC of native CNC, validating the presence of PLA in the sample (Fig. S3 in the Supporting Information). However, DSC failed to show the characteristic melting peak of PLA graft chains. The same phenomenon has been reported for in-situ polymerized cellulose nanocrystals-PLA nanomaterials [42] and could have been the result of the distance between the grafting spots on CNCs and/or the strong interaction between the graft chains and the CNC interface which results in the reduced flexibility of the chains and inability to crystallize properly.

CR – CNC nanocomposite films

In order to evaluate the properties of the cured CR samples, first, a curing system for CR was designed. CR is most commonly vulcanized using the micronized zinc oxide (ZnO) powder as the curing agent and magnesium oxide (MgO) as a scorch protector with or without curing rate modifiers e.g. tetramethyl thiuram disulfide (TMTD) or ethylene thiourea [43]. In this study a simplistic curing approach, which avoids the use of extra chemicals, was implemented to control the experimental factors. Moreover, some curing additives and accelerators could cause safety concerns. For instance, TMTD that is typically used as a curing rate modifier for CR triggers allergic reactions in applications that the final part comes in contact with humans (e.g. gloves) [44].

Preliminary experimentation was conducted to optimize the level of curing agents in CR nanocomposites, and a formulation composed of 100 phr CR, 2.5 phr of ZnO-N, and 2 phr of MgO-N was selected for the nanocomposite film fabrication very similar to that of Roy *et al* [45]. The curing mechanism for CR using this system is well documented [46]. It involves the reaction of ZnO with a labile chlorine group on the chain ~CH_2Cl and creation of an intermediate ~$C(H_2)OZnCl$ that will remove another labile chlorine atom from the next chain to form a crosslink between the two aforementioned chains and a $ZnCl_2$ molecule that is the byproduct and tends to make the compound scorchy (Fig. 1). However, the labile chlorine atom which is involved might be an allylic [46], or ordinary pendant chlorine next to the main chain [47]. The main role of MgO molecules is to react with $ZnCl_2$ molecules, and prevent the scorch and they are not involved in the main vulcanization mechanism. The addition of higher loadings of CNCs, or mCNCs (>3 wt%) was avoided because of the need for too much extra water needed for keeping down the viscosity and prolonged necessary drying time in excess of two days which is not acceptable in practical manufacturing processes. The aforementioned formulation was blended with the curing system, casted, dried, and cured. Films fabricated as such was then used to prepare test specimens.

Transmission electron microscopy

The TEM images of the control CR films, 3CNC, and 3mCNC containing no CNCs, 3 wt% virgin CNCs, and 3mCNCs, respectively are shown in Fig. 3. At higher magnifications (Fig. 3c, f, and i), small white dots

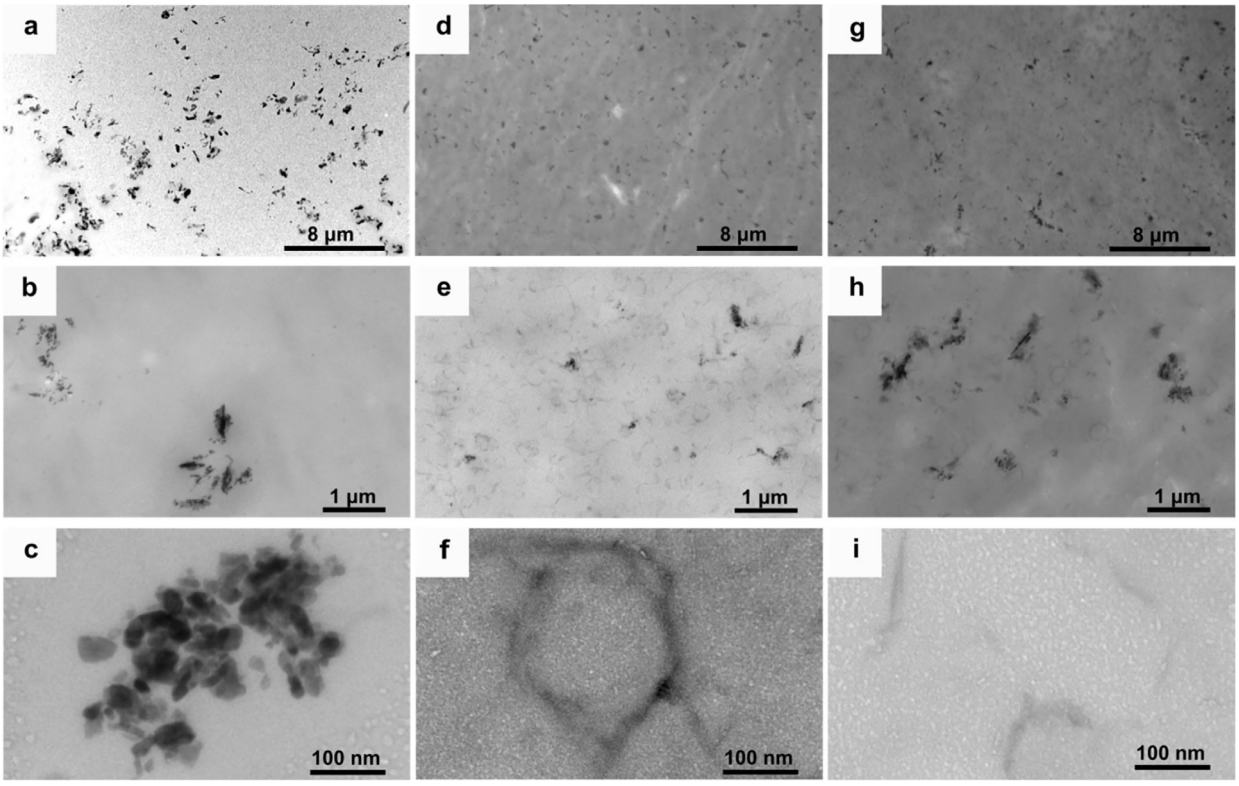

Fig. 3. TEM micrographs of: (a-d) chloroprene rubber control sample (CR) at different and increasing magnifications from (a) to (d); (e-h) chloroprene rubber with 3 wt% CNC at different and increasing magnifications from (e) to (h); (i-l) chloroprene rubber with 3 wt% of mCNC. at different and increasing magnifications from (i) to (l).

were noted that are suspected to be attributed to $ZnCl_2$ precipitation adducts as a result of the curing reactions in the rubber matrix. The left column of Fig. 3 (images a–c) shows the distribution of ZnO–N and MgO–N in CR (with no CNCs) with an increasing magnification from top to the bottom. Dark spots in these images are likely attributed to either ZnO–N or MgO–N, but it is not possible to differentiate between them. Overall, it appears that these curing agents are distributed well throughout the film (Fig. 3a) with some aggregation as noted from clusters at higher magnification (Fig. 3b and c).

The middle column in Fig. 3 (images d–f) is for the 3CNC sample, composed of the CR and 3 wt% of CNC. The comparison of the images 3(a) and 3(e) for the control and 3CNC samples, respectively showed that the larger clusters of ZnO–N/MgO–N have dispersed substantially indicating that the addition of CNC has improved the ZnO–N/MgO–N dispersion considerably. The virgin CNC nanoparticles show good dispersion in all the images (Fig. 3d–f). However, a closer look at the images (3e) and (3f) shows that there is a repeating polygonal pattern distributed across the samples.

The possible explanation is that during the film preparation, CNCs are first mixed in the aqueous media and because of their waterborne nature they were well dispersed in between the latex particles. After casting and during the film formation/drying process, CNCs are trapped between the coalescing particles. These particles cannot diffuse into the latex CR chains, which have formed the film and hence do not individually disperse in the rubber matrix. The vulcanization process further immobilizes the particles, and they appear as a polygonal structure in the crosscut samples prepared by the microtome. The structure is considered a partially structured network. Fig. 3f shows a typical single polygon in which the CNCs are tangentially extending outwards. The partially structured polygonal network could be considered as a slight agglomeration forming a continuous filler network, which can result in early percolation.

The right column of Fig. 3, which is for the 3mCNC nanocomposite films reinforced with 3 wt% mCNC, showed the individualized dispersion of ZnO–N/ MgO–N clusters (Fig. 3g). The dispersion of these curing agents was better than that of the control sample (Fig. 3a) and the number of the polygons (Fig. 3h and i) was much less than those of 3CNC samples (Fig. 3e and f). It can be noted that the majority of the mCNCs were dispersed well. This could be explained by their ability to interact with the polychloroprene chains inside the particles during the film drying process because of their better interfacial compatibility with CR.

Overall, enhanced dispersion of ZnO-N/ MgO-N was noted in the 3CNC and 3mCNC nanocomposite films compared to that of the control CR sample (Fig. 3d, g, and a respectively), which can be attributed to the interaction between CNC and mCNC with MgO-N and ZnO-N. For the ZnO/CNC interactions, Lafatshe et al [48] and Blanchard et al. [24] reported complex formation between CNCs and ZnO as the reason for the improved ZnO-N dispersion in nanocomposites. In the case of ZnO/mCNCs interactions, Anzlovar et al showed that ZnO retards the crystallization of PLA by interacting with the chains in a DSC analysis of ZnO/PLA nanocomposites [49]. So, mCNCs can interact with the ZnO surface via either the grafted PLAs or the bare -OH surface of the mCNCs.

In the case of MgO–N/CNC interactions, Mirtalebi et al. [50] investigated the nanocomposites of MgO/bacterial cellulose (BC) and found an interaction between them to be the reason for the reduced crystallinity of BC in DSC. This interaction can be the reason for the good dispersion of MgO-N in CNC/CR nanocomposites. In the case of MgO–N/mCNCs, similar interaction between MgO-N and PLA has been reported to be the reason for the reinforcement effect of MgO–N in PLA [51]. Moreover, Liang et al. [52] found the same interaction to be responsible for the change in an FTIR spectrum at a peak of 2994 cm^{-1} for the asymmetric vibration of the PLA chains on the MgO-N surface. So, mCNCs can interact with MgO-N surface via either the graft PLAs or the bare -OH

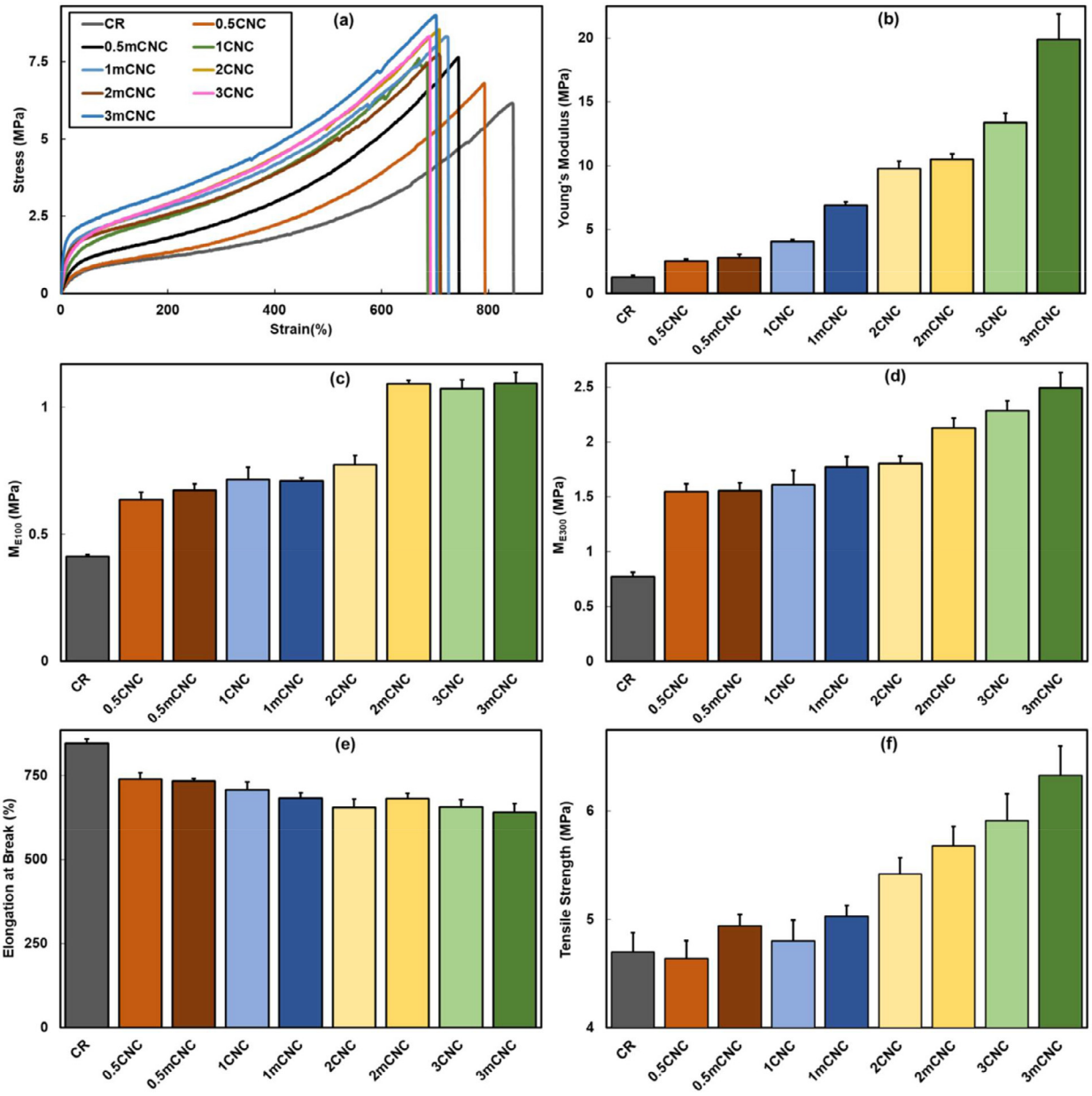

Fig. 4. Tensile properties of cast films (a) Typical stress–strain curves, (b) Young's modulus, (c) Modulus E100, (d) Modulus E300 (e) Elongation at break, (f) Tensile strength. CR has no cellulosic nanoparticles, and 0.5CNC, 1CNC, 2CNC, and 3CNC samples have 0.5, 1, 2, 3 wt% CNCs, and 0.5mCNC, 1mCNC, 2mCNC, and 3mCNC contain 0.5, 1, 2, 3 wt% mCNCs respectively.

moieties from the surface of the mCNCs. It is worth mentioning that the partial coverage of mCNCs by the graft PLA is the main reason for their good water dispersibility (Fig. S2a in the Supporting Information). Overall CNCs and mCNCs were dispersed well in CR at microscale but the latter dispersed even more so, (mostly individually, and they both improved the dispersion of ZnO-N, and MgO–N in CR considerably.

Tensile test

The control CR and its nanocomposite films constructed with the incorporation of both CNCs and mCNCs were defect-free, coherent, robust, and uniform. To evaluate the reinforcing capability of the CNCs and mCNCs and correlate with structures the structures observed via TEM, the tensile properties of the cured films were evaluated. Representative stress–strain curves for each sample is presented in Fig. 4a. It was noted that the Young's modulus started to exhibit improvement with the incorporation of only 0.5 wt% of CNCs to CR (Fig. 4b). A progressive enhancement in the Young's modulus was noted with a further increase in the loading of the CNCs, which was in line with a previous result [32] for green CR rubber and the expected trend [53].

In all cases the mCNC loaded samples had either similar (0.5 and 2 wt%) or higher moduli (1 and 3 wt%) compared to that of the corresponding pristine CNC loaded films. The slight increase can be attributed to the improved dispersion of the mCNCs in the CR matrix (Fig. 3i) as a result of better interaction between the PLA grafts and the CR. The improved dispersion reduces the overlap area of the mCNCs compared to that of CNCs with their polygonal pattern (Fig. 3e). This in turn increases the interfacial area of the particles whose role is to transfer the mechanical load applied to the matrix to the cellulosic nanoparticles and vice versa and improves the ability of the mCNCs to reinforce the rubber matrix. This is in line with the theoretical

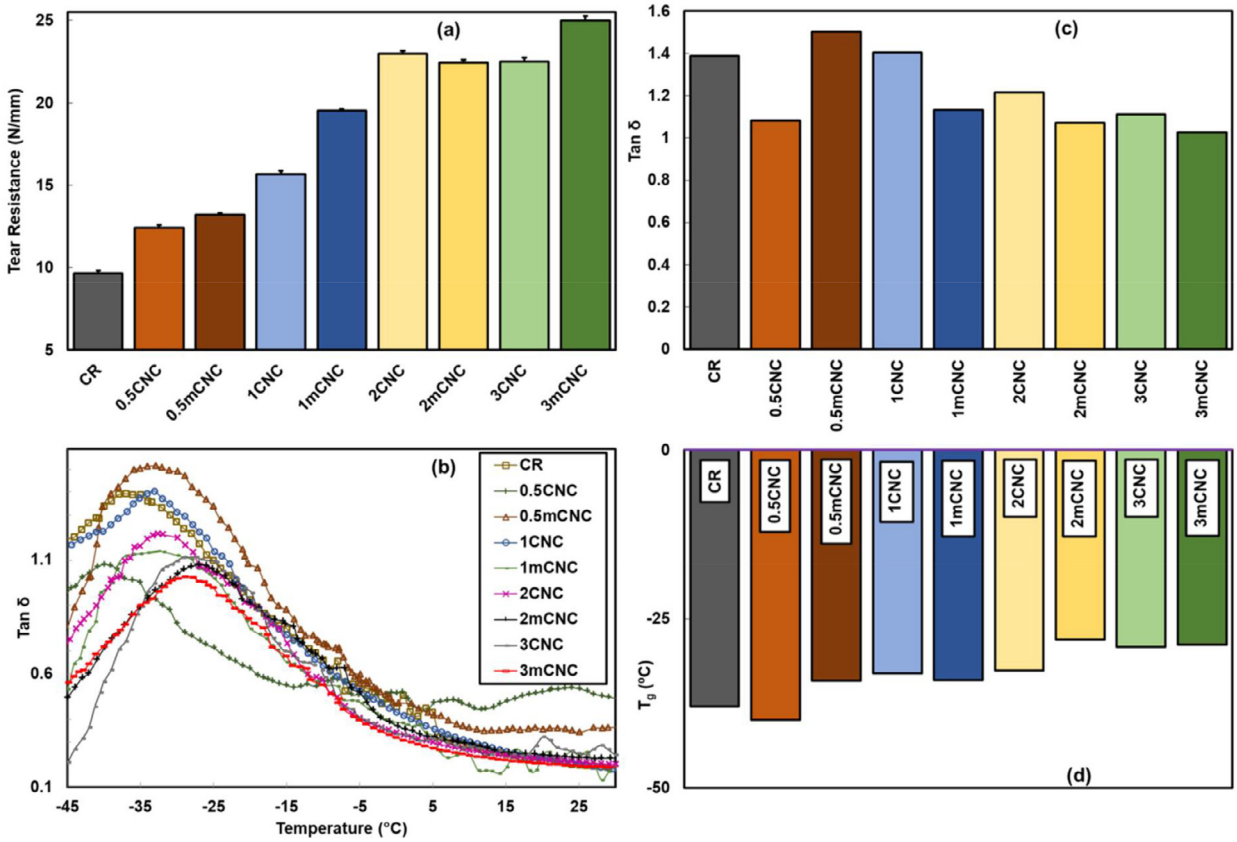

Fig. 5. a) Tear Resistance, b) Tan δ versus temperature, c) Tan δ data, d) T_gs for samples. CR has no cellulosic nanoparticles, and 0.5CNC, 1CNC, 2CNC, and 3CNC samples have 0.5, 1, 2, 3 wt% CNCs, and 0.5mCNC, 1mCNC, 2mCNC, and 3mCNC contain 0.5, 1, 2, 3 wt% mCNCs respectively.

predictions that the better the interfacial compatibility of the fillers is, the higher the composite modulus will be [27,53]. Additionally, the enhanced interfacial compatibility and possibly chain entanglement between the CNC with PLA grafts and the rubber can act as physical crosslinks and contribute to the observed higher modulus [54]. Similarly, in the mCNC fillers nanocomposites, the reduced overlap between particles and hence larger interaction area with the fillers, will act as extra physical crosslinking points that will in turn increase the modulus. The improved dispersion of ZnO–N/MgO–N could have also improved the cure by increasing the cross-linking density (Fig. S5 in Supporting Information). The largest increase in Young's modulus was for the sample with 3 wt% of mCNC, which increased from 1.3 MPa (for CR sample) to 19.9 MPa (3mCNC sample) as shown in Fig. 4b.

As expected, the elongations at break for the samples decreased upon the addition of the stiffer cellulosic nanoparticles from 846% for the control sample (CR) to the 3mCNC sample with the lowest elongation at break of 640%. Though the reduction is substantial, the lowest elongation at break (640%) is still acceptable for most practical applications (Fig. 4e). The tensile strength has also increased for all the samples with the highest increase (34%) obtained for 3mCNC (6.3MPa) which is 33% more than that of the control sample (4.7 MPa; Fig. 4f). Overall, the tensile strength, and modulus increased for all samples with the addition of CNCs and mCNCs and the latter gave marginally higher values without much damage to the elongation at break for either case.

Tear test

The effect of CNC fillers on the cut growth and propagation of the rubber nanocomposite films under tension was evaluated using the trouser cut (Die T) method in accordance with ASTM D624-12. The addition of cellulosic nanoparticles increased the tear propagation resistance of the samples in all cases (Fig. 5a). The tear resistance displayed progressive enhancement up to 2 wt% of the CNC or mCNC loading and levels off. The highest increase was observed for 3mCNC sample with 25 N/mm compared to that of the control sample (CR) of 9.7 N/mm which was a 158% increase. These results indicate that the use of CNCs as a reinforcing agent and as a tear resistance enhancer of CR films is appealing for a range of dipped goods. This was shown in other rubber films and sheets as well [24,39,74]. For instance, it can prolong the service life of disposable gloves considerably.

Dynamic mechanical analysis

The dynamic mechanical properties of the nanocomposites were also characterized by DMA. The storage modulus E' (Fig. S6 in Supporting Information) samples show glassy, glass transition, and rubbery states. Above the glass transition temperature (T_g) including at ambient temperature, the vulcanizates are in the rubbery state. Storage modulus is a measure of the degree of elasticity and the moduli follow the same trend as of the crosslink density which is shown in the swelling data (Figs. S5 and S6 in Supporting Information, respectively). In the glassy state, the moduli of the nanocomposites show a good increase with the addition of the cellulosic nanoparticles, indicating reinforcement in agreement with the tensile test result.

The shape of damping curves can give some information about the reinforcement mechanisms. In the typical curves for the samples (Fig. 5b), the Tan δ peak heights (Fig. 5c) was less than 1.5 for all the samples at their corresponding T_g, which shows that the energy absorption characteristics of the samples are minimal as expected for elastomers. Samples that contain the fillers exhibited a further reduced Tan δ with the minimum for 3mCNC (1.027) and hence the highest elastic nature. Also the curves for the samples with nanocellulosic particles are sharper (half-peak width) compared to that of the control CR which is another sign of good interaction between the nanoparticles and the matrix [55].

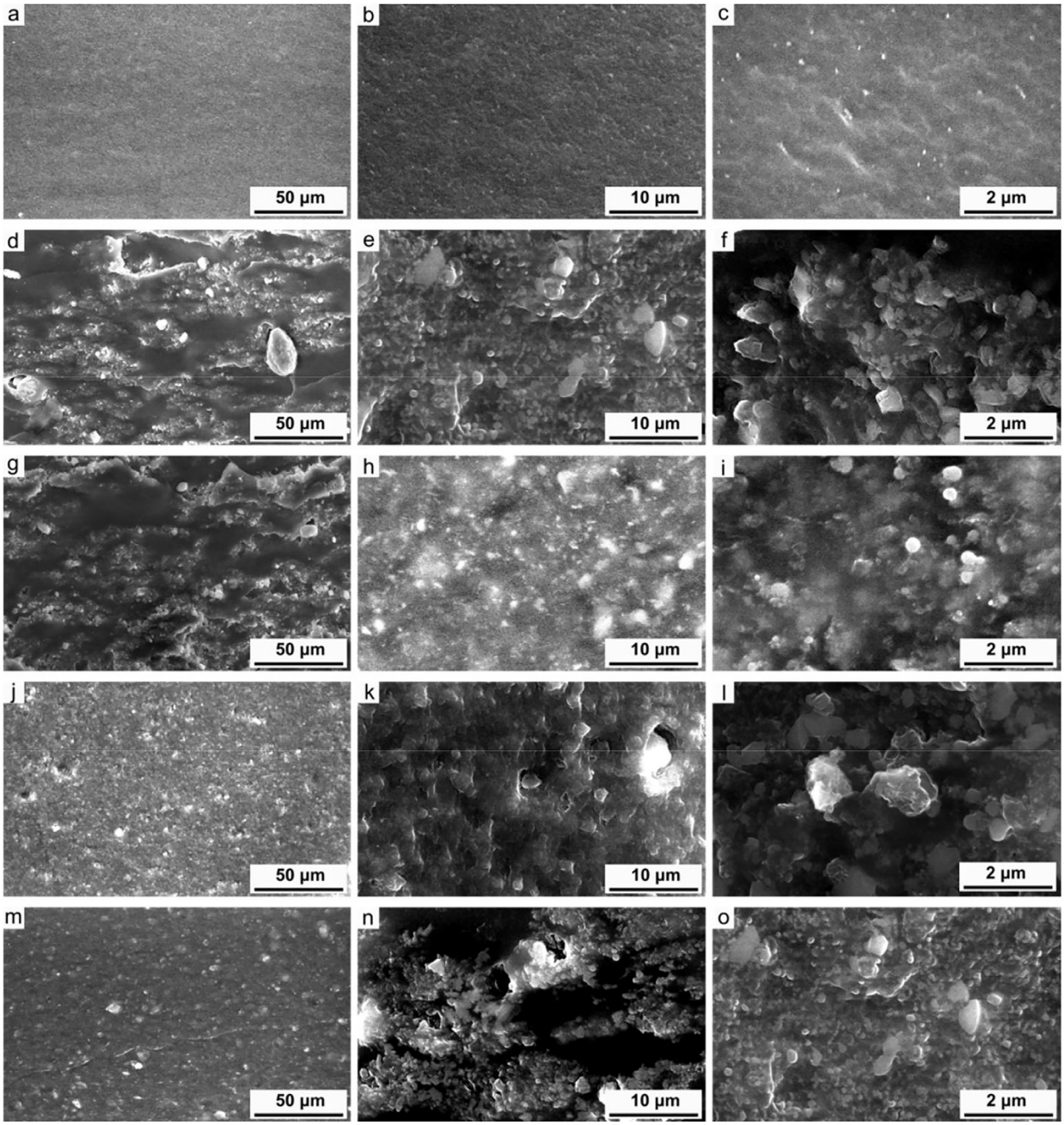

Fig. 6. SEM micrographs of: (a–c) chloroprene rubber control sample(CR) at different and increasing magnifications from a to c; (d–f) chloroprene rubber with 0.5 wt% CNC at different and increasing magnifications from d to f; (g–i) chloroprene rubber with 0.5 wt% mCNC at different and increasing magnifications from (g–i); (j-l)chloroprene rubber with 3 wt% CNC at different and increasing magnifications from j to l; and (m-o) chloroprene rubber with 3 wt% mCNC at different and increasing magnifications from m to o (magnifications are the same within each column) More images for samples 1CNC, 1mCNC, 2CNC, and 2mCNC are available in the supporting information.

As the T_g shift can be used as a measure of the degree of interaction between the components, its values are shown in Fig. 5d. As expected, good interaction between the cellulosic nanoparticles and the matrix induces T_g confinement. This results in less free volume and the suppression of the mobility of rubber chains and causes an upward shift in the location of the peaks (T_g) to higher temperatures (Fig. 5d), which has happened for all the samples except 0.5CNC. The reason for this interaction might be the hydrogen bonding between hydroxyl groups on the cellulosic nanoparticles surface and the chlorine atoms of the CR which has been proposed to occur between –OH groups of the silica surface and CR too [56,57]. Also, the filler network of CNCs formed as observed in the TEM images (Fig. 3) can restrict the mobility of rubber network, and better dispersion of ZnO–N/MgO–N might have caused a higher crosslinking density which is supported by the swelling data (Fig. S5 in Supporting Information)

In the case of 0.5CNC sample, it is worth mentioning that although the decrease in T_g is minimal, a similar anomalous decrease in T_g has been reported for PMMA-alumina composites [58] and other systems [59,60], and the effect of filler on T_g has been modeled [61]. Possible explanations that match our system and offered for similar systems have been: (i) The effect of the residual surfactants of the parent latex [62] (in our case the CR latex surfactants) that might have preferential adsorption on the CNCs and result in an increase in the free volume for the polymer matrix; (ii) the interaction of ZnO–N and MgO–N with the

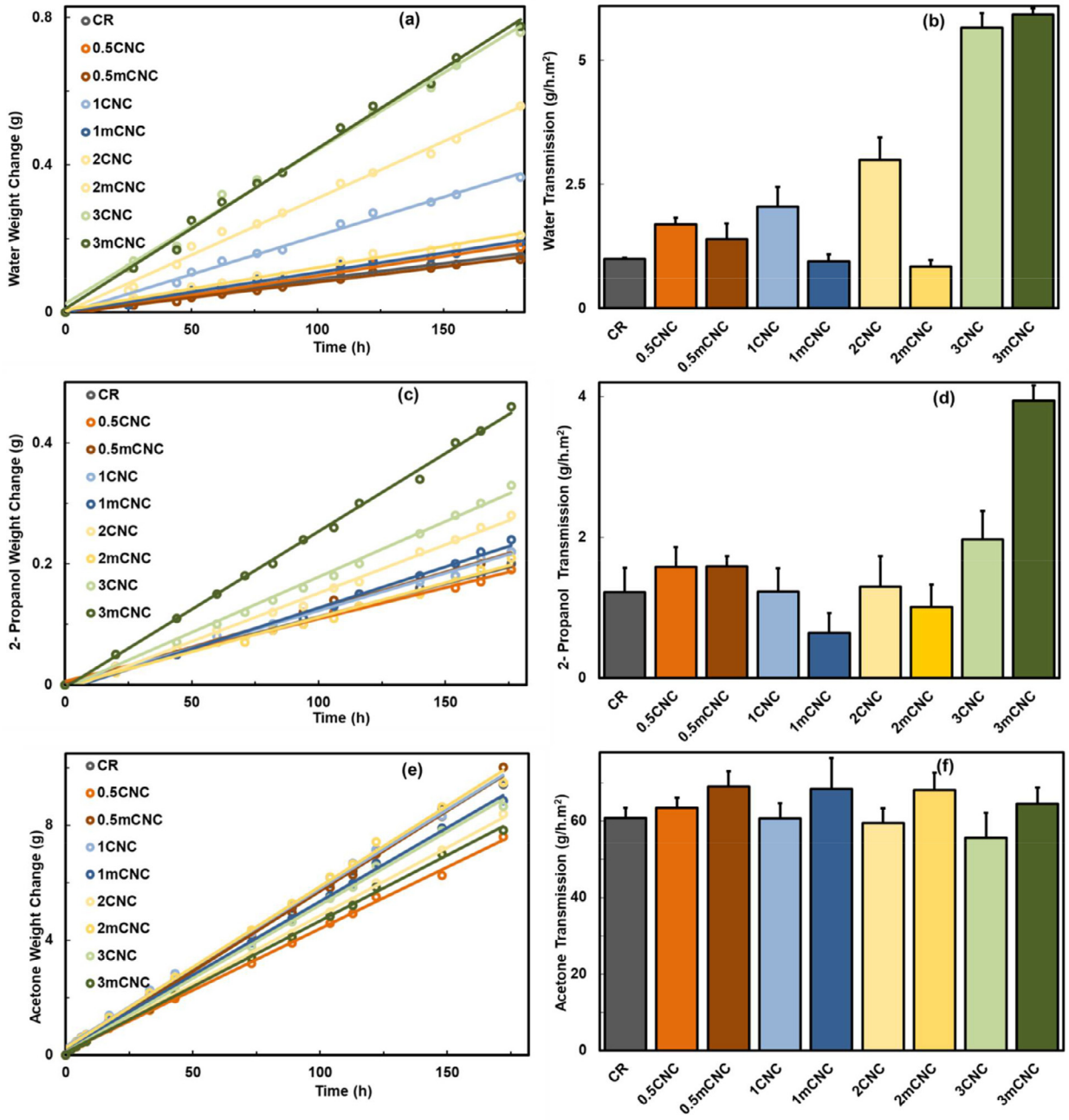

Fig. 7. (a)Water vapor transmission test results, and (b) the water vapor transmission rates for different samples; (c) 2-Propanol vapor transmission test results, and (d) 2-propanol vapor transmission rates for different samples; (e) Acetone vapor transmission results, and (f) the acetone transmission rates for different samples. CR has no cellulosic nanoparticles, and 0.5CNC, 1CNC, 2CNC, and 3CNC samples have 0.5, 1, 2, 3 wt% CNCs, and 0.5mCNC, 1mCNC, 2mCNC, and 3mCNC contain 0.5, 1, 2, 3 wt% mCNCs respectively.

surface of the CNCs that can result in their sticking to CNCs and reduce the number of ZnO-N and MgO-N in the matrix. As these particles have a high surface-to-weight ratio their absence in the bulk of polymer matrix results in less bound rubber, more free volume and hence less T_g confinement. Overall, the addition of more than 0.5 wt% of either CNCs or mCNCs increases the storage modules, and T_g, and increases the elastic nature of the nanocomposite.

Scanning electron microscopy

We also used SEM to investigate the fractured cross-sectional surfaces after the tear test specimens. Fig. 6 shows the SEM micrographs of CR and its nanocomposites with 0.5, 3 wt% of CNC, and mCNC. Images (a) to (c) show the interface for the CR control sample which is clear and almost flat. On the contrary, row 2 (images d to f) and row 3 (images g to i) from the top, which correspond to CR nanocomposites with 0.5 wt% of CNC and mCNC, respectively show some fibrillar/nodular structures which were protruding out of the fracture surface. These bumps were numerous and smaller in size for the third row (0.5mCNC) compared to those of the second row (0.5CNC). The presence of these bumps on the surface indicated good interfacial adhesion between the rubber matrix and the CNCs as well as mCNCs [63] that resulted in reinforcement. For row 4 and row 5, which are for samples 3CNC, and 3mCNC, respectively, similar coverage can be seen that indicates the same reinforcement mechanism. Comparison of images (l) and (o) (Fig. 6) for 3CNC, and 3mCNC, respectively, showed that the nodules on the surface

are a bit smaller in size for that of 3mCNC, which can indicate a finer dispersion of the reinforcing particle and is in agreement with the results of TEM offered earlier. More images for samples 1CNC, 1mCNC, 2CNC, and 2mCNC are available in the supporting information (Fig. S6). Overall, the SEM images are in agreement with the TEM results indicating the possibility of effective reinforcement of the CR via the CNCs and mCNCs.

Solvent vapor transmission

The barrier properties of dipped goods are important for a range of applications. For instance, gloves used as PPEs are expected to provide protection against particulates and impermeability to solvents such as 2-propanol which is the main ingredient of disinfectants used against a range of bacteria and possibly viruses. The perspiration entrapped in the gloves is a major issue with their use and causes discomfort [64] and skin crack formation on fingers, exposing the body to more harm. This can also cause a human error for the people wearing the gloves [65] with grave consequences in some cases. The main solution has been to absorb water using the powder inside the gloves. For instance, Fraga et al. [66] studied the water absorption behavior of gloves to reduce the sweat trapped in the gloves and keeping the gloves workable. The same study compared the water absorption behaviour of nitrile, chloroprene, and vinyl gloves and detected no water absorption for CR gloves. Therefore having a higher water permeability of gloves might be of interest in glove applications [67,68,74] as this can reduce the moisture by letting it pass through the gloves, evaporate, and reduce the sweat content inside.

CNCs are hydrophilic and have been shown to increase the water permeability of NR and SBR with possible applications in gloves moisture removal [39]. We performed the transmission test with water, 2-propanol, and acetone using the cup method [40]. Makela et al [69,70] have reported the permeability data for nitrile gloves. It is worth mentioning that the mass transfer mechanism through a nanocomposite membrane is usually a mix of the Fickean diffusion and surface flow. In the Fickean mechanism, a diffusing molecule is absorbed in the membrane matrix surface on one side and diffuses through the matrix to the boundary at a lower concentration. In the second mechanism for surface flow, the aforementioned matrix contains fillers and in addition to the Fickean diffusion the filler surface acts as a canal to move the diffusant. Thus the diffusant is (i) adsorbed by the filler surface (ii) moved along that surface towards the boundary at a lower concentration, and (iii) desorbed from the filler surface to the matrix at a lower concentration. The mass flux is the sum of the Fickean diffusion and the surface flow. Thus an impermeable polymer to a chemical species can become permeable by adding a filler that can provide a surface that can adsorb the chemical and provide a surface flow for it [71].

Fig. 7 shows the results for the vapor transmission tests on water (images a and b), 2-propanol (images c and d), and acetone (images e and f). For water, Fig. 7a and b show the typical water transmission line, and the water transmission rate for different samples respectively. In the case of the samples with CNCs addition (0.5CNC, 1CNC, 2CNC, and 3CNC in Fig. 7b), a clear increase in the transmission rate by increasing the filler loading was noted. This might be attributed to the presence of light percolation caused by the polygonal pattern shown in the TEM images (Fig. 3e and f), and at higher loadings of CNCs higher surface area results in more surface flow and percolation. The result is in agreement with the observed increase in the transmission rate of water upon the addition of CNC to NR and SBR [39]. However, when mCNC was added progressively to the nanocomposite, the water transmission rate did not increase initially and remained about the same up to 2 wt% and it showed an increase only at 3wt% of mCNC that could be attributed to the percolation of the individually dispersed particles. The percolation threshold of CNC was calculated to be about 3 phr [39], and for the 3mCNC that is above the threshold, the percolated mCNC network can show surface flow for water molecules through the surface of the mCNC particles in the CR matrix.

Fig. 7c and d show the typical transmission line and the transmission rates of 2-propanol through the various samples. It was observed that for samples with up to 2 wt% CNCs or mCNCs (0.5CNC, 1CNC, 2CNC, 0.5mCNC, 1mCNC, and 2mCNC) the transmission rate of 2-propanol did not change. However, for the sample with 3% mCNC the transmission rate shows an appreciable increase. Sato et al [72] studied the effect of swelling of PLA in various solvents on its crystallinity and reported that PLA is swollen in 2-propanol by 8.3 wt%. Therefore the increase in the transmission rate of 2-propanol can be attributed to the same percolation mentioned for water but here via a transfer pathway through the 2-propanol-swollen graft PLA chains on the mCNCs.

Fig. 7e and f show the typical acetone transmission curve and the transmission rate for different samples. In this case, the transmission is almost the same for all the samples. For acetone, the solubility parameter is 19.7 $Mpa^{1/2}$ which is very close to that of CR (19.8 $Mpa^{1/2}$) [73]. This results in good compatibility and absorption of acetone in CR and its diffusion through CR via a Fickean diffusion mechanism. The addition of the CNCs does not increase the vapor transmission rate, and even acts as a barrier for the mass transfer, which might be the reason for a rather small drop in the overall transmission rate (Samples 0.5CNC, 1CNC, 2CNC, and 3CNC). The mCNCs loaded samples show a slight increase in the transmission rate compared to the CNCs loaded samples that might be attributed to PLA grafts (20.3 $Mpa^{1/2}$) that can swell in acetone and slightly increase the overall diffusion, but the increase is still not significant compared to the Fickean contribution in the transmission mechanism.

In short, the addition of CNCs creates partially structured network that provides surface diffusion for some chemicals like water and 2-propanol and hence decelerated increase in the permeability for the whole range. However, for chemicals that can diffuse on the surface of mCNCs, a boost in permeability was noticed only after adding mCNCs at a level more than the percolation threshold of ~3wt%.

Conclusions

The results of this study show that CR nanocomposites films reinforced with either pristine CNCs or modified CNCs via surface grafting of PLA (mCNCs) are strong and coherent with very good tear and tensile strengths, modulus, and acceptable elongation at break. Overall, the property enhancements were better for the mCNCs as compared to those of the pristine CNCs. TEM studies showed that for CNC/CR nanocomposites, there were partially structured (polygonal) network in which the CNCs made the walls and do not diffuse into the internal compartments, which resulted in weak percolation at even low CNC loadings, while for mCNC/CR nanocomposites, the mCNCs were mostly individually dispersed and showed percolation at 3 wt%. The SEM images were in agreement with the TEM results indicative of reinforcements for both CNCs and mCNCs. The incorporation of CNCs and mCNCs in CR caused water permeability increase in the nanocomposite films. While the increase was incremental for the CNC/CR nanocomposites due to the partially structured network, it did not show an increase for mCNC/CR until it reached the percolation limit of ~3 wt%. Overall, the constructed CR based nanocomposite films have great potential for high performance medical gloves or other dipped products.

Declaration of Competing Interest

The authors declare that they have no conflict of interest.

Acknowledgments

Financial support from Natural Resources Canada through the Clean Growth Program is gratefully acknowledged. Donation of the native CNC material by CelluForce Inc. is greatly appreciated.

Supplementary materials

Supplementary material associated with this article can be found, in the online version, at doi:10.1016/j.jcomc.2020.100009.

References

[1] Marinović-Cincović M, Marković G, Jovanović V, Samaržija-Jovanović S, Budinski-Simendić J, Marinović-Cincović M, et al. Polychloroprene rubber-based nanoblends: preparation, characterization and applications n.d. https://doi.org/10.1007/978-3-319-48720-5_8.

[2] MG Maya, SC George, T Jose, L Kailas, S Thomas, Development of a flexible and conductive elastomeric composite based on chloroprene rubber, Polym. Test 65 (2018) 256–263, doi:10.1016/j.polymertesting.2017.12.006.

[3] SZ Salleh, MZ Ahmad, H Ismail, Properties of natural rubber/recycled chloroprene rubber blend: effects of blend ratio and matrix, Procedia Chem. 19 (2016) 346–350, doi:10.1016/j.proche.2016.03.022.

[4] Napolitano M.Respirator System for use with a hood or face mask. US 4899740, 1990.

[5] Gyeong E, Lim K, Park JM, Cheon Y, Jeong MJ, Choi S-K, et al. Chloroprene rubber modified by nanosilica for performance adhesion strength 2018. https://doi.org/10.1080/15421406.2018.1456113.

[6] R. Suntako, Effect of zinc oxide nanoparticles synthesized by a precipitation method on mechanical and morphological properties of the CR foam, vol. 38 (2015).

[7] S Mostoni, P Milana, B Di Credico, M D'arienzo, R Scotti, Zinc-based curing activators: new trends for reducing zinc content in rubber vulcanization process, Catalysts 9 (2019), doi:10.3390/catal9080664.

[8] Acikgoz C, Üniversitesi B, Acikgoz C, Sahbaz DA, Kockar OM. ZnO nanoparticles bonded to SiO2 filler as a curing accelerator in cold vulcanizing adhesives2017;131. https://doi.org/10.12693/APhysPolA.131.200.

[9] Xu Z, Zheng L, Wen S, Liu L. Graphene oxide-supported zinc oxide nanoparticles for chloroprene rubber with improved crosslinking network and mechanical properties 2019. https://doi.org/10.1016/j.compositesa.2019.105492.

[10] KM. Anderson, Zinc loaded clay as activator in sulfur vulcanization: a new route for zinc oxide reduction in rubber compounds, Prevent. Sch. Fail. 51 (1986) 49–51.

[11] K Roy, MN Alam, SK Mandal, SC Debnath, Development of a suitable nanostructured cure activator system for polychloroprene rubber nanocomposites with enhanced curing, mechanical and thermal properties, Polym. Bull. 73 (2016) 191–207, doi:10.1007/s00289-015-1480-7.

[12] SP Thomas, EJ Mathew, V Marykutty C, Nanomodified fillers in chloroprene-rubber-compatibilized natural rubber/acrylonitrile-butadiene rubber blends, J. Appl. Polym. Sci. 124 (2012) 4259–4267, doi:10.1002/app.35406.

[13] S Kar, AK. Bhowmick, Nanostructured magnesium oxide as cure activator for polychioroprene rubber, J. Nanosci. Nanotechnol. 9 (2009) 3144–3153, doi:10.1166/jnn.2009.005.

[14] C Swaroop, M. Shukla, Polylactic acid/magnesium oxide nanocomposite films, for food packaging applications, 21st Int. Conf. Compos. Mater. Xi'an, 20-25th August 2017, 2017.

[15] Noori AJ, Kareem A. The effect of magnesium oxide nanoparticles on the antibacterial and antibiofilm properties of glass-ionomer cement 2017. https://doi.org/10.1016/j.heliyon.2019.e02568.

[16] R Sengupta, S Chakraborty, S Bandyopadhyay, S Dasgupta, R Mukhopadhyay, K Auddy, et al., A short review on rubber/clay nanocomposites with emphasis on mechanical properties, Polym. Eng. Sci. 47 (2007) 1956–1974, doi:10.1002/pen.20921.

[17] A Das, KW Stöckelhuber, R Jurk, G Heinrich, Routes to rubber nanocomposites, Macromol. Symp. 291–292 (2010) 95–105, doi:10.1002/masy.201050512.

[18] K Roy, SC Debnath, P Potiyaraj, A critical review on the utilization of various reinforcement modifiers in filled rubber composites, J. Elastomers Plast. 52 (2020) 167–193, doi:10.1177/0095244319835869.

[19] Das A, Reny Costa F, Wagenknecht U, Heinrich G. Nanocomposites based on chloroprene rubber: effect of chemical nature and organic modification of nanoclay on the vulcanizate properties 2008. https://doi.org/10.1016/j.eurpolymj.2008.08.025.

[20] K Roy, MN Alam, SK Mandal, SC Debnath, Silica-coated nano calcium carbonate reinforced polychloroprene rubber nanocomposites: influence of silica coating on cure, mechanical and thermal properties, J. Nanostruct. Chem. 6 (2016) 15–24, doi:10.1007/s40097-015-0174-x.

[21] ZM Abbas, M Tawfilas, MM Khani, K Golian, ZM Marsh, M Jhalaria, et al., Reinforcement of polychloroprene by grafted silica nanoparticles, Polymer 171 (2019) 96–105, doi:10.1016/j.polymer.2019.03.031.

[22] K Subramaniam, A Das, D Steinhauser, M Klüppel, G Heinrich, Effect of ionic liquid on dielectric, mechanical and dynamic mechanical properties of multi-walled carbon nanotubes/polychloroprene rubber composites, Eur. Polym. J. 47 (2011) 2234–2243, doi:10.1016/j.eurpolymj.2011.09.021.

[23] A Malas, CK. Das, Effect of graphene oxide on the physical, mechanical and thermo-mechanical properties of neoprene and chlorosulfonated polyethylene vulcanizates, Compos. Part B Eng. 79 (2015) 639–648, doi:10.1016/j.compositesb.2015.04.051.

[24] Blanchard R, Ogunsona E, Hojabr S, Berry R, Mekonnen T, Ogunsona EO, et al. Synergistic crosslinking and reinforcing enhancement of rubber latex with cellulose nanocrystals for glove applications n.d. https://doi.org/10.1021/acsapm.9b01117.

[25] T Mekonnen, MA Dubé, Special Issue "renewable polymers: processing and chemical modifications.", Processes 7 (2019) 398, doi:10.3390/pr7070398.

[26] P Panchal, TH. Mekonnen, Tailored cellulose nanocrystals as a functional ultraviolet absorbing nanofiller of epoxy polymers, Nanoscale Adv. 1 (2019) 2612–2623, doi:10.1039/c9na00265k.

[27] EO Ogunsona, P Panchal, TH Mekonnen, Surface grafting of acrylonitrile butadiene rubber onto cellulose nanocrystals for nanocomposite applications, Compos. Sci. Technol. 184 (2019), doi:10.1016/j.compscitech.2019.107884.

[28] J Tang, J Sisler, N Grishkewich, KC Tam, Functionalization of cellulose nanocrystals for advanced applications, J. Colloid Interface Sci. 494 (2017) 397–409, doi:10.1016/j.jcis.2017.01.077.

[29] M Ly, T. Mekonnen, Cationic surfactant modified cellulose nanocrystals for corrosion protective nanocomposite surface coatings, J. Ind. Eng. Chem. (2019), doi:10.1016/j.jiec.2019.12.014.

[30] EO Ogunsona, R Muthuraj, E Ojogbo, O Valerio, TH Mekonnen, Engineered nanomaterials for antimicrobial applications: a review, Appl. Mater. Today 18 (2020) 100473, doi:10.1016/j.apmt.2019.100473.

[31] F Fahma, N Hori, T Iwata, A Takemura, Preparation and characterization of polychloroprene nanocomposites with cellulose nanofibers from oil palm empty fruit bunches as a nanofiller, J. Appl. Polym. Sci. 131 (2014), doi:10.1002/app.40159.

[32] H Eslami, C Tzoganakis, TH Mekonnen, Surface graft polymerization of lactic acid from the surface of cellulose nanocrystals and applications in chloroprene rubber film composites, Cellulose (2020), doi:10.1007/s10570-020-03167-w.

[33] OK Ha, A. Raghu, Prognosis now the world's hospitals are running out of vital rubber gloves, Bloomberg (2020).

[34] BC WS. Latex - WorkSafeBC 2020.

[35] Torres M. Can you wash and reuse disposable gloves? | HuffPost Canada Home & Living. Huffingt Post 2020.

[36] BM Trinh, T. Mekonnen, Hydrophobic esterification of cellulose nanocrystals for epoxy reinforcement, Polymer 155 (2018), doi:10.1016/j.polymer.2018.08.076.

[37] EO Ogunsona, P Panchal, TH Mekonnen, Surface grafting of acrylonitrile butadiene rubber onto cellulose nanocrystals for nanocomposite applications, Compos. Sci. Technol. 184 (2019), doi:10.1016/j.compscitech.2019.107884.

[38] ASTM A. ASTM E96 / E96M-05, Standard Test Methods for Water Vapor Transmission of Materials, ASTM International. ASTM Int, 2016, doi:10.1520/E0096_E0096M-16.

[39] JM Jardin, Z Zhang, G Hu, KC Tam, TH Mekonnen, Reinforcement of rubber nanocomposite thin sheets by percolation of pristine cellulose nanocrystals, Int. J. Biol. Macromol. 152 (2020) 428–436, doi:10.1016/j.ijbiomac.2020.02.303.

[40] Duc Thuan B, Yonghui W, Kian Jon C, Kim Choon N. Evaluating water vapor permeance measurement techniques for highly permeable membranes. vol. 47. 2015.

[41] N Eidelman, CG. Simon, Characterization of combinatorial polymer blend composition gradients by FTIR microspectroscopy, J. Res. Natl. Inst. Stand. Technol. 109 (2004) 219–231, doi:10.6028/jres.109.014.

[42] C Miao, WY Hamad, In-situ polymerized cellulose nanocrystals (CNC)—poly(L-lactide) (PLLA) nanomaterials and applications in nanocomposite processing, Carbohydr. Polym. 153 (2016) 549–558, doi:10.1016/j.carbpol.2016.08.012.

[43] K Berry, M Liu, K Chakraborty, N Pullan, A West, C Sammon, et al., Mechanism for cross-linking polychloroprene with ethylene thiourea and zinc oxide, Rubber Chem. Technol. 88 (2015) 80–97, doi:10.5254/rct.14.85986.

[44] Rudzki E. Allergy to tetramethylthiuram disulfide, a component of pesticides and rubber. vol. 5. 1998.

[45] K Roy, MN Alam, • Swapan, K Mandal, • Subhas, C Debnath, Development of a suitable nanostructured cure activator system for polychloroprene rubber nanocomposites with enhanced curing, mechanical and thermal properties, Polym. Bull. 73 (2016) 191–207, doi:10.1007/s00289-015-1480-7.

[46] W Hofmann, Rubber Technology Handbook, Hanser Publishers, Munich; Vienna; New York, 1989 Reprint.

[47] H Desai, KG Hendrikse, CD Woolard, Vulcanization of polychloroprene rubber. I. A revised cationic mechanism for ZnO crosslinking, J. Appl. Polym. Sci. 105 (2007) 865–876, doi:10.1002/app.23904.

[48] K Lefatshe, CM Muiva, LP Kebaabetswe, Extraction of nanocellulose and in-situ casting of ZnO/cellulose nanocomposite with enhanced photocatalytic and antibacterial activity, Carbohydr. Polym. 164 (2017) 301–308, doi:10.1016/j.carbpol.2017.02.020.

[49] A Anžlovar, A Kržan, E Žagar, Degradation of PLA/ZnO and PHBV/ZnO composites prepared by melt processing, Arab. J. Chem. 11 (2018) 343–352, doi:10.1016/j.arabjc.2017.07.001.

[50] SS Mirtalebi, H Almasi, M Alizadeh Khaledabad, Physical, morphological, antimicrobial and release properties of novel MgO-bacterial cellulose nanohybrids prepared by in-situ and ex-situ methods, Int. J. Biol. Macromol. 128 (2019) 848–857, doi:10.1016/j.ijbiomac.2019.02.007.

[51] Y Zhao, B Liu, H Bi, J Yang, W Li, H Liang, et al., The degradation properties of MgO whiskers/PLLA composite in vitro, Int. J. Mol. Sci. Article (2018), doi:10.3390/ijms19092740.

[52] H Liang, Y Zhao, J Yang, X Li, X Yang, Y Sasikumar, et al., Fabrication, crystalline behavior, mechanical property and in-vivo degradation of poly(l–lactide) (PLLA)–magnesium oxide whiskers (MgO) nano composites prepared by in-situ polymerization, Polymers 11 (2019) 1123, doi:10.3390/polym11071123.

[53] Y Gao, J Liu, J Shen, L Zhang, Z Guo, D Cao, Uniaxial deformation of nanorod filled polymer nanocomposites: a coarse-grained molecular dynamics simulation †, Phys. Chem. Chem. Phys. 16 (2014) 16039, doi:10.1039/c4cp01555j.

[54] Vacatello M. Monte Carlo simulations of polymer melts filled with solid nanoparticles 2001. https://doi.org/10.1021/ma0015370.

[55] X Cao, C Xu, Y Wang, Y Liu, Y Liu, Y Chen, New nanocomposite materials reinforced with cellulose nanocrystals in nitrile rubber, Polym. Test. 32 (2013) 819–826, doi:10.1016/j.polymertesting.2013.04.005.

[56] P Sae-oui, C Sirisinha, U Thepsuwan, K Hatthapanit, Dependence of mechanical and aging properties of chloroprene rubber on silica and ethylene thiourea loadings, Eur. Polym. J. 43 (2007) 185–193, doi:10.1016/j.eurpolymj.2006.10.015.

[57] BP Kapgate, C Das, A Das, D Basu, S Wiessner, U Reuter, et al., Reinforced chloroprene rubber by *in situ* generated silica particles: evidence of bound rubber on the silica surface, J. Appl. Polym. Sci. 133 (2016), doi:10.1002/app.43717.
[58] P Rittigstein, JM. Torkelson, Polymer-nanoparticle interfacial interactions in polymer nanocomposites: Confinement effects on glass transition temperature and suppression of physical aging, J. Polym. Sci. Part B Polym. Phys. 44 (2006) 2935–2943, doi:10.1002/polb.20925.
[59] Robertson CG, Lin CJ, Rackaitis M, Roland CM. Influence of particle size and polymer-filler coupling on viscoelastic glass transition of particle-reinforced polymers n.d. https://doi.org/10.1021/ma7022364.
[60] S-J Li, H-J Qian, Z-Y Lu, A simulation study on the glass transition behavior and relevant segmental dynamics in free-standing polymer nanocomposite films, Soft Matter 15 (2019) 4476–4485, doi:10.1039/C9SM00267G.
[61] KJ Lee, DK Lee, YW Kim, W-S Choe, JH Kim, Theoretical consideration on the glass transition behavior of polymer nanocomposites, J. Polym. Sci. Part B Polym. Phys. 45 (2007) 2232–2238, doi:10.1002/polb.21178.
[62] L Chen, JM. Torkelson, Tuning the Tg-confinement effect in thin polymer films via minute levels of residual surfactant which “cap” the free surface, Polymer 87 (2016) 226–235, doi:10.1016/j.polymer.2016.02.009.
[63] Bascom WD. Scanning electron microscopy of rubber tear. 1977.
[64] Bishu RR, Chin A. No TitleInner gloves: how good are they? 1998.
[65] V Gnaneswaran, B Mudhunuri, RR Bishu, A study of latex and vinyl gloves: performance versus allergy protection properties, Int. J. Ind. Ergon 38 (2008) 171–181, doi:10.1016/j.ergon.2007.10.027.
[66] F Fraga, E Rodríguez-Núñez, S Díaz de Freijo, JM Martínez-Ageitos, F Suárez-Pereiro, Studies of absorption in sanitary protective gloves, J. Test Eval. 43 (2015) 20130316, doi:10.1520/JTE20130316.
[67] CN Peiss, WC. Randall, The effect of vapor impermeable gloves on evaporation and sweat suppression in the Hand1, J. Investig. Dermatol. 28 (1957) 443–448, doi:10.1038/jid.1957.58.
[68] DH Branson, L Abusamra, C Hoener, S Rice, Effect of glove liners on sweat rate, comfort, and psychomotor task performance, Text Res. J. 58 (1988) 166–173, doi:10.1177/004051758805800307.
[69] EA Mäkelä, S Vainiotalo, K Peltonen, The permeability of surgical gloves to seven chemicals commonly used in hospitals, Ann. Occup. Hyg. 47 (2003) 313–323, doi:10.1093/annhyg/meg044.
[70] EA. MAKELA, Permeation of 70% isopropyl alcohol through surgical gloves: comparison of the standard methods ASTM F739 and EN 374, Ann. Occup. Hyg. 47 (2003) 305–312, doi:10.1093/annhyg/meg043.
[71] Kao MB, Sircar S. Nanoporous carbon membranes for separation of gas mixtures by selective surface flow. vol. 85. 1993.
[72] S Sato, D Gondo, T Wada, S Kanehashi, K Nagai, Effects of various liquid organic solvents on solvent-induced crystallization of amorphous poly(lactic acid) film, J. Appl. Polym. Sci. 129 (2013) 1607–1617, doi:10.1002/app.38833.
[73] M van Duin, H Dikland, A chemical modification approach for improving the oil resistance of ethylene-propylene copolymers, Polym. Degrad. Stab. 92 (2007) 2287–2293, doi:10.1016/j.polymdegradstab.2007.04.018.
[74] E. Ogunsona, S. Hojabr, R. Berry, T. Mekonnen, Int. J. Biol. Macromol. (2020). In press, doi:10.1016/j.ijbiomac.2020.07.202.